Development of a selective chloride sensing platform using a screen-printed platinum electrode

Hugo Cunha-Silva, M. Julia Arcos-Martinez

www.elsevier.com/locate/talanta

PII: S0039-9140(18)31276-1
DOI: https://doi.org/10.1016/j.talanta.2018.12.008
Reference: TAL19356

To appear in: *Talanta*

Received date: 25 September 2018
Revised date: 3 December 2018
Accepted date: 5 December 2018

Cite this article as: Hugo Cunha-Silva and M. Julia Arcos-Martinez, Development of a selective chloride sensing platform using a screen-printed platinum electrode, *Talanta,* https://doi.org/10.1016/j.talanta.2018.12.008

Development of a selective chloride sensing platform using a screen-printed platinum electrode

Hugo Cunha-Silva and M. Julia Arcos-Martinez*

Departamento de Química, Facultad de Ciencias, Universidad de Burgos, Plaza Misael Bañuelos s/n, 09001 Burgos, Spain
e-mail: jarcos@ubu.es

Abstract

A new and selective voltammetric method for chloride determination is proposed, based on platinum and chloride interactions. A screen-printed platinum electrode (SPPtE) functions as a sensing platform, which promotes the formation of chloro-adsorbed species on the electrode surface, acting as an effective means of anion-determination in several matrices. The pretreatment of the SPPtE and careful control of the cathodic stripping voltammetric parameters yielded a well-defined electrochemical signal. This cathodic peak was due to the adsorption of chlorine, which had previously been oxidized from chloride anions in the initial anodic deposition step. It offers a simple, low-cost, fast, reproducible (RSD < 6%) and precise method for selective chloride determination, with limit of detection of 0.76 mM, and a sensitivity of -24.147 μA mM^{-1} for a broad determination range of up to 150 mM. Chloride determination was correctly performed with single drops of environmental, pharmaceutical and food samples. In addition, the sensor was successfully adapted as a flexible screen-printed platinum electrode sensor using Gore-Tex® as support for printing.

Graphical Abstract:

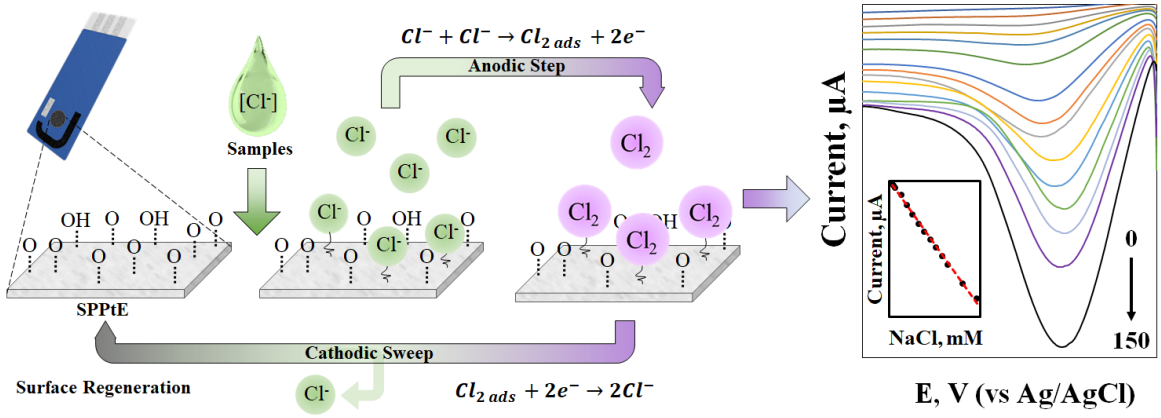

Keywords:

Chloride; Platinum electrode surface; Cathodic stripping voltammetry; Screen-printed electrode; Flexible sensor.

1. Introduction

Chloride ion concentration is an important parameter in various environmental [1–3], pharmaceutical and food-related fields [4,5]. Chloride also has a significant role in biology and medicine, as an essential electrolyte that maintains corporal homeostasis, functioning as a diagnostic indicator of various conditions and diseases. The chloride content of sweat samples is widely analyzed for the diagnosis of cystic fibrosis (CF) [6]. At normal levels, sweat chloride can reach a maximum of 40 mmol L^{-1}, exceeding 70 or 80 mmol L^{-1} in CF positive individuals [6–11]. As the most abundant ion in perspiration, chloride is also a potential biomarker for electrolyte loss in endurance activities [12,13]. A further example is the diagnosis of chloride levels that are outside the normal plasma range of 96 – 106 mmol L^{-1} indicating conditions of hypo or hyperchloremia [14,15]. Also present in urine, at concentrations ranging between 110 and 250 mmol L^{-1}, chloride anion levels can provide information on kidney malfunctions [16,17]. Lower levels of chloride anions are also present in the cerebrospinal fluid of patients with amyotrophic lateral sclerosis [18].

The Mohr volumetric method [19], potentiometric ion selective electrodes (ISE) [20–23], and more recently ion-chromatographic analysis [24,25] are all current standards for chloride determination. Likewise, resonance light scattering [26], turbidimetry [27], colorimetry [28,29], fluorescence [30] and spectrophotometric [31,32] methods, have all been developed. Additionally, some papers published in recent years [33–49] have described several screen-printed electrode (SPE) based electrochemical sensors that perform chloride analysis. The clear advantages of this type of disposable platforms are the low-cost of the materials in use, the possibility of on-site testing, and simple handling of the electrode modifications for their analysis [49]. The majority of studies on chloride determination using SPE are based on the formation of stable compounds between silver and chloride [33,34,40,47,50]. The Nernstian shift of a control species voltammetric peak has also been used for chloride determination, since the pseudo-reference SPE Ag/AgCl is affected in the presence of this anion [35–38]. Some of these SPE-based sensors printed on flexible substrates are designed to determine sweat chloride. The excellent properties of fabric-based SPEs have also been applied to the development of wearable sensors [35,50].

Even with the interesting results obtained from the above-mentioned methodologies, significant disadvantages still exist. Despite offering continuous measurements, potentiometric methods are time-consuming and require stabilization steps, complicating any routine use. Moreover, ISEs usually have a limited lifetime, requiring regular electrode replacement. Some of the SPE-based sensors that have been described [35,48] need control species, adding possible interferents to the analysis, and requiring sample preparation. Silver-based sensors [33,34,36,40,47,50] present problems such as their complex preparation, electrode fouling, impractical continuous measurement, and reduced concentration ranges.

The demand for an efficient analytical tool calls for the development of new, fast and simple methods of chloride determination. A novel Pt-based SPE sensor is therefore proposed in this paper, in response to the problems found with silver-based SPEs.

Platinum (Pt) is a noble metal, with extensive applications in the electrochemical field. Pt electrode properties are strongly affected by the presence of chloride ions, particularly when high anodic potentials are applied during the experiments [51–57]. At these potentials, the chloride anions that are specifically adsorbed on the Pt surfaces block the adsorption of oxygen and chlorine gas discharge occurs [57]. Indeed, exhaustive

research has already been focused on chloride behavior on Pt surfaces and the fundamentals of its interactions [51–60].

In this study, the feasibility of an electrochemical sensor, using a screen-printed platinum working electrode (SPPtE) is investigated, as an alternative to other approaches for the detection of chloride ions in matrices of a different nature. Although chloride-Pt interactions have been already studied, to the best of our knowledge, only one paper describes those interactions in the context of chlorine gas determination [60]. This method achieved a detection limit of only 1.93 mM, and a linear range of up to 42 mM that is unsuitable for direct analysis of some chloride samples.

The SPPtE-based sensor developed in this work, uses cathodic stripping voltammetry (CSV) to improve chloride detection. Thus, a simple, fast, low-cost, disposable SPPtE-based sensor was successfully tested for chloride determination in environmental, pharmaceutical and food samples. In addition, a flexible SPPtE sensor was developed that could form the basis for the development of a wearable sensor to monitor the chloride levels of human sweat.

2. Experimental Section

2.1. Chemicals and reagents

Human plasma, L(-)-malic acid, sodium pyruvate, and D(+)-glucose monohydrate, alanine, aspartic acid, glutamic acid, phenylalanine, glycine, propionic acid, folic acid, iodide, isovaleric acid, leucine, tryptophan, valine, butyric acid, nickel nitrate hexahydrate, calcium sulfate dihydrate, and isobutyric acid, were purchased from Sigma-Aldrich (Steinheim, Germany). L-histidine monohydrochloride monohydrate, sulfuric acid, urea, ascorbic acid, ammonia, sodium phosphate dibasic dihydrate, sodium phosphate monobasic dihydrate, magnesium nitrate, copper(II) sulfate pentahydrate, potassium chloride, and potassium nitrate, were obtained from Merck (Darmstadt, Germany). L-lactic acid (85%), succinic acid, anhydrous citric acid, ortho-phosphoric acid (85%), tyrosine, iron ammonium sulfate hexahydrate, cadmium nitrate tetrahydrate, potassium bromide, sodium bicarbonate, potassium sulfate, sodium fluoride, iron ammonium sulfate hexahydrate, and sodium chloride were purchased from Panreac-Applichem (Darmstadt, Germany). Creatinine was obtained from Cromatest (Barcelona), uric acid from Alfa Aesar and acetic acid from VWR (France).

Commercial wholemeal biscuits, chicken stock, and saline solution were obtained from local markets.

Human sweat and urine samples were collected from healthy volunteers and stored at -20ºC before use.

Human plasma, was prepared at 0.05 % (w/v) in a phosphate buffer (0.31 mM, pH 6.2) and spiked with two levels of sodium chloride, of 47 mM and 125 mM, to simulate conditions of hypo and hyperchloremia, respectively.

Synthetic sweat was formulated, as described elsewhere [13,61], according to the median levels of the compounds found in real human perspiration (Table A1).

All reagents were of analytical grade and all solutions were prepared with Milli-Q water (Millipore, Bedford, USA).

The inks used for the fabrication of the SPEs, Electrodag PF-407 A (carbon ink), Electrodag 6037 SS (silver/silver chloride ink), and Electrodag 452 SS (dielectric ink), were supplied by Achenson Colloiden (Scheemda, Netherlands). Polymer platinum ink (C2050804P9) was obtained from Gwent Group (Mamhilad, United Kingdom). Polyester films (PET) of 0.5 mm thickness (HIFI Industrial Film, Dardily, France) and Gore-Tex® PACLITE® Shell 2-Layer Ripstop Nylon (from Rockywoods Fabrics LLC, Loveland, USA) were used as the printing substrates.

2.2. Apparatus

Voltammetric measurements were performed using a PalmSens® portable electrochemical potentiostat with the PS Trace 4.2 program (PalmSens® Instruments BV, Houten, The Netherlands).

The potentiometric analysis was performed with a pH & Ion-Meter GLP 22+, connected to a chloride ion selective electrode 96 52 C, from CRISON Instruments, S.A. (Barcelona, Spain).

The conventional three-electrode system was obtained from BASI bioanalytical systems (West Lafayette, USA). It consisted of three electrode cells, namely a platinum electrode with a diameter of 1.6 mm (MF-2013), a platinum wire electrode (CHI115), and a silver/silver chloride electrode (MF-2025), used as the working, counter, and reference electrodes, respectively.

Microscopy imaging and elemental composition analysis were performed using a scanning electron microscope (SEM) JEOL JSM-6460LV with an INCA elementary X-ray analysis system Oxford Instruments

(Abingdon-on-Thames, UK). The X-ray analysis was performed at three different zones of each working electrode with a zoom of x500.

2.3. SPE manufacturing and preparation

The SPE systems were fabricated by sequential ink layer deposition on PET and Gore-Tex® supports, previously heated and held at a temperature of 120º for 2h. SPE manufacturing was completed following previously described procedures [62]. Briefly, silver and silver/silver chloride inks, cured at 120 °C for 20 min, were used to print the conductive tracks and the reference electrodes, respectively. The counter electrode was then printed with carbon ink and cured at 60 °C for 30 min. Next, platinum ink was screen-printed and cured at 80 °C for 30 min. to define the Pt working electrodes (SPPtE) (Area = 12.56 mm^2). Finally, dielectric ink, which defines the final geometry of the three electrodes, was printed and cured under the same conditions.

Before the chloride analysis, each electrode was electrochemically polished in KNO_3 0.1 M, by applying 5 cyclic voltammetric scans from -0.20 to -1.50 V at 0.05 V s^{-1} (Fig. A1).

2.4. Cyclic voltammetric measurements

The screening of electrochemical behavior of chloride at SPPtE, was carried out using cyclic voltammetric (CV) experiments, performed by drop casting 200 µL of supporting electrolyte (phosphate buffer, 0.31 mM, pH 6.2), containing 5, 10, 20, 30, 60, 80, and 100 mM NaCl, onto the electrode surface. Voltammograms were recorded, between -0.70 V and 1.30 V (vs SPE Ag/AgCl) at 0.1 V s^{-1}.

Randles-Sevcik CV experiments, were performed by drop-casting 200 µL of supporting electrolyte containing 60 mM NaCl, onto the electrodic system, from 0.40 to 1.30 V (vs SPE Ag/AgCl), at the following scan-rate values: 0.025, 0.050, 0.075, 0.100, 0.150 and 0.200 V s^{-1}.

The experiments using the conventional three-electrode cell system, were performed from 0.40 to 1.30 V (vs Ag/AgCl) in a cell containing 10 mL of supporting electrolyte, and the desired chloride concentration, spiked from a stock solution of NaCl 3 M, at 0.1 V s^{-1}.

2.5. Cathodic stripping voltammetry for chloride determination

The cathodic stripping voltammetric (CSV) experiments were performed by drop casting 200 µL of supporting electrolyte containing different concentrations of NaCl onto the electrodic surface. A first deposition step at 1.50 V was applied over 15 seconds, followed immediately (equilibration time 0 s) by a cathodic linear sweep voltammetric scan, from 1.11 to 0.10 V at a scan rate of 0.20 V s^{-1}, returning a reduction peak at 0.80 V.

2.6. Chloride ion selective electrode measurement

A chloride ion selective electrode (Cl – ISE) was the reference method used to corroborate the voltammetric results. The experiments were performed in stabilization mode and the potential value recorded after measurement stabilization. According to the supplier, chloride standards from 0.5 to 60 mM of KCl were prepared in KNO_3 0.01 M. Calibration curve (log [KCl] (mM) vs potential (mV)), was used to determine the chloride content in samples.

3. Results and discussion

3.1. Chloride voltammetric peak screening

As previously mentioned, several authors have described specific interactions between chloride and platinum surfaces, once this anion leads to the inhibition of redox processes [52], competing with oxides and protons that are usually adsorbed [55].

Confirmation of those sorts of interactions at the SPPtE was carried out by screening the voltammetric peak in the presence of chloride through CV scans. In Fig. 1, numerous peaks appear within the CV experimental data. Special attention was given to the cathodic peak developed at 1.0 V, as its potential remained stable, showing a relation with chloride concentrations. This is in agreement with the findings of Kuhn and Wright for platinum electrode behavior in strong chloride solutions [51]. This peak may be related with the chlorine gas generated on the working electrode surface. No stable oxidation signal was observed in the CV scans, to pair it with the reduction signal, so several experiments, were performed to determine the cause of the reduction. The results obtained for potential sweeps, by means of CSV performed from 1.3 to 0 V, were therefore analyzed.

3.2. CSV setting for chloride quantification

CSV was found to be the ideal technique to follow the reduction peak developed in the presence of chloride ions. Previous experiments have shown that the current signal is notably increased when an anodic pretreatment step is performed before the cathodic potential sweep. In doing so, the influence of both anodic potential ($E_{dep.}$) and time deposition ($t_{dep.}$) pretreatment can be considered. In this study, an E_{dep} of 1.5 V was applied over 15 s as the optimal CSV conditions (Fig. A2).

3.3. SPPtE electropolishing

When assessing the performance of the sensor for chloride determination, under the previously adjusted conditions, it was found that the voltammetric reduction peaks were irreproducible and unstable. An electropolishing step of the SPPtE in 0.1 M KNO_3 was therefore performed (*Section 2.3. SPE Manufacturing and Preparation*). The cyclic voltammograms obtained for electropolishing step, exhibits a different behavior in the first scan, since the reduction peak developed at -1.0 V disappeared over repeated KNO_3 scans (Fig A1).

With the purpose of detecting modifications in the typical proton and oxygen adsorption zones on Pt surfaces, the effect of this step was studied in acidic media [63]. Thus, when 0.1 M H_2SO_4 was used as a supporting electrolyte, the untreated SPPtE exhibited a flat CV profile, with low current densities and imperceptible signals. Contrasting data were found when using an electropolished working electrode (SPPtE/EP), which recorded increased current outputs and a well-marked CV profile, displaying the expected peaks shapes and positions usually found for a Pt surface (Fig. A3). This treatment generates a higher number of active sites for the reaction on the electrode surface. These data might be related with the presence of a polycrystalline nanosurface of platinum available to interact with reactants [51,55,63], as a result of the elimination of Pt ink impurities.

The data obtained in the X-ray elemental composition analysis of the SPPtE/EP surface (see Appendix B), confirmed the increase of a more electroactive surface, revealing a 15 % increment in oxygen composition, when compared with an untreated SPPtE (Table 1). The chloride reduction peak was also shifted from 1.0 to

0.8 V when the CSV experiments were performed, which confirmed that the chloride redox process occurred more easily and extensively on a treated surface, rather than on an untreated SPPtE.

The chloride voltammetric peak current was remarkably increased at SPPtE/EP and the number of scans improved the anion determination. Five cycles were selected for the electropolishing step, as lower deviations were found between replicas (Fig. A1).

An additional study, using a conventional (not screen-printed) three-electrode cell system with a Pt working electrode, was performed in the presence of chloride, before and after KNO_3 electropolishing. As observed using a SPPtE, under the CV conditions employed for chloride voltammetric peak screening (CV from -0.7 to 1.3 V, at different chloride concentrations, in phosphate buffer, 0.31 mM, pH 6.2), the conventional Pt electrode developed a well-defined reduction peak at 1.0 V (vs Ag/AgCl), which current is related with chloride concentrations (Fig. A4). Nevertheless, the electropolishing of this conventional Pt electrode, displayed a different behavior to those observed at the SPPtE, developing a flat behavior over the five scans (Fig. A5). This Pt surface also behaved differently in CSV experiments, originating weak reduction peaks that can barely be related with chloride concentrations. Even though poor linearity was found for the chloride calibration at this conventional Pt surface, KNO_3 electropolishing also increased the current output for the cathodic peaks (Fig. A6).

As previously mentioned, the Pt ink is also crucial for chloride determination, as the conventional metallic Pt electrode proved itself ineffective at obtaining a satisfactory response in the presence of the anion. Therefore, all the experiments conducted for the characterization, application and validation of the proposed sensor, were performed with previously electropolished SPPtEs. This step, performed just before the first utilization, demonstrated stable measurements.

3.4. Electrochemical mechanism for CSV chloride reduction peak

It has been demonstrated that the reduction peaks observed in CSV experiments can be related with chlorine evolution; however, it involves a complex mechanism. In fact, many processes may occur on the electrode surface involving both faradaic and non-faradaic contributions. A chemisorption electrochemical mechanism is proposed for a better understanding of the voltammetric reduction peak and its generation in chloride containing-media. The mechanism may rely on the formation of chloro-complexes on the Pt surface, which

are oxidized during the anodic pretreatment, applied just before the cathodic sweep. Somewhat conflicting information exists regarding the type of complexes formed; nevertheless, there is agreement that an oxide layer deposited on the Pt surface will favor chloride complexation with the metal. Some of those complexes are described as $PtCl^-$, $PtCl_2$, $PtCl_4^{2-}$ and $PtCl_6^{2-}$ [51–57]. Other studies, in agreement with the results found using the proposed system, have indicated the presence of strongly adsorbed chlorine atoms in the electrode reaction mechanism [58–60].

X-ray analyses of the different steps of sensor operation for chloride analysis was used to evaluate changes in the SPPtEs surface composition (see Appendix B). The wt % of each element was compared on various surfaces: untreated SPPtE (identified as *SPPtE* in table 1), after the KNO_3 electropolishing treatment (identified as SPPtE/*EP* in table 1), when submitted to an anodic treatment at a E_{dep} of 1.5 V applied during 15 s under different chloride concentrations in the solution (identified as SPPtE/EP/E_{dep} *0, 10 and 150 mM NaCl* in table 1), and after the cathodic sweep, also at different chloride concentrations (identified as SPPtE/EP/E_{dep} *0, 10 and 150 mM NaCl/CSV* in table 1). The untreated *SPPtE* presented a small percentage of oxygen, limiting the formation of chloro-adsorbed complexes that originated small voltammetric reduction peaks. The oxide layer was increased after the electropolishing step (*SPPtE/EP*), which prompted extensive interaction between chloride and Pt, resulting in improved sensitivity to the anion. This is also noticeable for the Pt oxide peak current, which is improved at a EP/SPPtE (Fig. A3).

Moreover, when the anodic deposition step was performed without the cathodic potential sweeping (*SPPtE/EP/*E_{dep} *NaCl)*, a wt % of chloride was found on the electrode surface. However, when chloride was absent in the anodic deposition step, no compositional change was perceptible in comparison with the *SPPtE/EP* surface. In this step, surface chloride and oxygen also appeared to be related with the lowest wt % of oxygen that was present when the chloride concentration was increased. This observation lends support to the idea that the formation of chloro-adsorbed complexes requires a previously formed oxide layer, which promoted interaction between anions and the Pt surface. The X-ray elemental analysis, summarized in Table 1, also offers information on the electrochemical reduction of adsorbed chlorine gas, confirming the disappearance of chloride from the Pt surface, after the cathodic potential sweep (*SPPtE/EP/*E_{dep} *10 and 150 mM NaCl/CSV*).

The X-ray data showed that the mechanism relies on chloride complexation at the electropolished Pt surface, where its oxidization releases chlorine gas during the anodic step (Eq. 1). During this step, gas bubble emerges from the sample, revealing that chlorine generation was occurring at these high potentials. Subsequently, the electrochemically generated chlorine gas was reduced to chloride anions during the cathodic potential sweeping (Eq. 2); regenerating the oxide layer at less positive potentials and recycling the Pt surface for a new reaction. It is suggested that this behavior results from a nondissociative adsorption of chlorine gas on the Pt electrode surface, which is followed by electron transfer [60].

$$2Cl^- \rightarrow Cl_{2\,ads} + 2e^- \quad (1)$$

$$Cl_{2\,ads} + 2e^- \rightarrow 2Cl^- \quad (2)$$

Murugappan and co-workers proposed a similar mechanism for the detection of chloride gas on a Pt microdisk. Their conclusion was that chlorine gas must partition into the liquid phase before chlorine reduction occurs at the electrode surface [60]. In our system, the chlorine gas is formed on the working electrode and partitioning may also occur. Even so, nondissociative chlorine gas absorption may be favored, as the chlorine is generated *in situ* and is then reduced to its corresponding anions.

Fig. 2 shows SEM SPPtE imaging of a rough surface, constituted by spherical microstructures of platinum that are homogeneous throughout the different steps of the analysis. This rough surface also contributes to the nondissociative chlorine gas absorption mechanism, playing an important role in sensor performance. So, it can be assumed that the successive steps converged in the improved effectiveness of the SPPtE to react, rather than alter its surface morphology. Furthermore, the Randles-Sevcik equation, produced a non-linear relation; indicating that this mechanism is not controlled by diffusion, with the possible involvement of adsorbed intermediates (Fig. A7) [64].

3.5. SPPtE-based sensor characterization

If an analytical method is to be characterized, it is important to establish its precision in terms of reproducibility and repeatability. Reproducibility was calculated taking into account calibration curves registered by the different sensors (inter-sensors), and repeatability with one single sensor (intra-sensor). The CSV responses of the SPPtE sensor to chloride concentrations over a range of 150 mM are shown in Fig. 3 a and b. After 150 mM, a loss on linearity was observed, leading to saturation of the sensor. The average value

of the voltammetric peak currents of several samples was used to construct the calibration curves. The reproducibility associated with the slopes of these calibrations, in terms of relative standard deviation (RSD) was 5.80% (n=7), and a sensitivity of -24.147 µA mM^{-1} was achieved. In terms of repeatability, a single SPPtE-based sensor maintained a stable slope over six successive calibrations, each constructed of sixteen measurements (Fig. A8). Despite the disposable characteristics of the SPEs, considering that the evaluation of each concentration corresponds to one experiment, each sensor was able to perform an average of 118 ± 5 reliable experiments in synthetic chloride samples. A limit of detection (LOD) of 0.76 mM, was obtained by LOD $=3S_{x/y}/b$, where $S_{x/y}$ is the estimated standard deviation of the lowest concentration that was detected, and b is the average slope of the calibration curves [65,66].

3.6. Analysis of interferences

It is important to check the specificity of the SPPtE to chloride, when other halides are present at the same concentration levels. Therefore, fluoride, bromide and iodide were evaluated and their voltammetric behaviors were analyzed. Only bromide originated a reduction peak at 0.60 V under the optimized experimental conditions. This reduction peak can hinder the chloride peak when bromide is present in concentrations above 10 mM. So, despite the different peak potential, the determination of chloride by using the SPPtE-based sensor in high bromide content samples should be reconsidered, in view of the false positive results that can emerge. Nonetheless, bromide is not expected to occur in such high concentrations in most samples.

Moreover, other anions and several cations, organic acids, carbohydrates, aminoacids and nitrogen compounds, found in biological samples, were carefully analyzed at three distinct concentrations (Table A1). None of the components under consideration, showed a major interference with the sensor operation for chloride determination. However, biological matrices present various organic substances that can cause electrode passivation, reducing the availability of sites for the formation of chloride surface complexes.

3.7. SPPtE-based sensor application and validation

The SPPtE-based sensor can be a useful tool to determine chloride content in several matrices. It offers reliable performance for selective analysis with an absence of any relevant interferents. Efficient determination of this anion in environmental, pharmaceutical, and food samples was successfully performed.

Some of these samples required a pretreatment step, such as centrifugation, dilution and calcination, in order to fit the sample into the calibration range, or as previously mentioned, to avoid electrode poisoning (Table A2).

Real sample analysis was performed using the standard addition method, except in the analysis of human sweat, the peak current value of which was introduced in the calibration curves previously built from synthetic sweat, given the limited availability of real samples.

The SPPtE sensor results, shown in table 2, corroborated with potentiometric measurements of chloride-ion selective electrode (Cl-ISE), confirmed the viability and applicability of the voltammetric sensor to determine the chloride content of several sample types.

3.7.1. Sensor application for sweat analysis

Over the past few years, the application of sensorial platforms specifically for the determination of sweat chloride has been under investigation, for non-invasive analysis of this electrolyte [29,34,35,38], which is useful in CF disease diagnosis and for monitoring electrolyte loss during exercise [6–12]. Thus, considering the suitability of the sensor in this field, special attention was given to sweat samples.

In vitro studies, using synthetic sweat samples, shown in Fig. 4, yielded well defined CSV peaks showing excellent linear correlation with chloride concentrations (R^2 = 0.9997), and a sensitivity of -13.618 µA mM^{-1}. Moreover, the electrodic system was printed on Gore-Tex®, which could be considered as a proof-of-concept for sweat analysis, given that flexible substrates are required for the development of wearable devices. This device, presented good linearity and analogous performances to those obtained with the rigid substrate (Fig. 4).

Comparing the CSV peaks for synthetic sweat with those of the supporting electrolyte (Fig. 3), a lower slope of the calibration curves was found. These data may be an indicator of electrode poisoning, that agree with the work of Polta and Johnson, who observed that electrochemical detection of aminoacids and carbohydrates was not successful using Pt electrodes, due to the accumulation of adsorbed reaction products under anodic potentials at Pt surfaces [67]. Nevertheless, a good linear relation was obtained in the range of interest to determine chloride concentration in real human sweat samples. Thus, the height of the reduction peaks was interpolated in the previously built synthetic sweat calibration curve, detecting a chloride value of 30.76 ±

3.61 mM in the human sweat sample, which is in agreement with the value obtained using the Cl-ISE (Table 2).

4. Conclusions

A new electrochemical chloride sensor has been developed, based on recognized interactions between the chloride anion and the platinum electrode surfaces. The formation of surface chloro-complexes at the SPPtE working electrode surface are oxidized in a primary anodic step to chlorine gas. This gas is strongly adsorbed onto the Pt surface and reduced in the cathodic scan, originating reduction peaks that present a linear relation with chloride concentration in the matrix. Its large linear range (0.76 to 150 mM) fits ideally with the chloride concentrations that can be found in several types of samples, making this sensor a versatile analytical tool. The device has proven to be a low-cost, non-invasive, simple, reusable and reproducible method for chloride determination. Furthermore, the high specificity of its analysis has revealed that the reaction between platinum and chloride prevails in the presence of numerous compounds, allowing selective chloride determination in different types of environmental, pharmaceutical, and food samples. Additionally, the printing technique is easily transferable to a flexible Gore-Tex® SPPtE-based sensor that future research could further adapt, as a wearable non-invasive tool for CF diagnosis and for monitoring electrolyte loss in endurance activities.

Acknowledgements

This work was supported by the Spanish Ministry of Science and Innovation (MICINN), Ministry of Economy and Competitiveness (MINECO) and the European Regional Development Fund (FEDER) (TEC20013-40561-P and MUSSEL RTC-2015-4077-2). Hugo Cunha-Silva would like to acknowledge funding from the Spanish Ministry of Economy (BES-2014-068214).

References

[1] J.A. Hern, G.K. Rutherford, G.W. Vanloon, Determination of chloride, nitrate, sulphate and total sulphur in environmental samples by single-column ion chromatography, Talanta. 30 (1983) 677–682. doi:10.1016/0039-9140(83)80155-6.

[2] F.J. Millero, R. Feistel, D.G. Wright, T.J. McDougall, The composition of Standard Seawater and the definition of the Reference-Composition Salinity Scale, Deep. Res. Part I Oceanogr. Res. Pap. 55 (2008) 50–72. doi:10.1016/j.dsr.2007.10.001.

[3] J.A. Morales, L.S. De Graterol, J. Mesa, Determination of chloride, sulfate and nitrate in groundwater samples by ion chromatography, J. Chromatogr. A. 884 (2000) 185–190. doi:10.1016/S0021-9673(00)00423-4.

[4] A.C. Galvis-Sánchez, I. V. Tóth, A. Portela, I. Delgadillo, A.O.S.S. Rangel, Monitoring sodium chloride during cod fish desalting process by flow injection spectrometry and infrared spectroscopy, Food Control. 22 (2011) 277–282. doi:10.1016/j.foodcont.2010.07.022.

[5] R. Pérez-Olmos, R. Herrero, J.L.F.C. Lima, M.C.B.S.M. Montenegro, Sequential potentiometric determination of chloride and nitrate in meat products, Food Chem. 59 (1997) 305–311. doi:10.1016/S0308-8146(96)00263-4.

[6] P.M. Farrell, T.B. White, N. Derichs, C. Castellani, B.J. Rosenstein, Cystic Fibrosis Diagnostic Challenges over 4 Decades: Historical Perspectives and Lessons Learned, J. Pediatr. 181 (2017) S16–S26. doi:10.1016/j.jpeds.2016.09.067.

[7] M.I. Barrio Gómez de Agüero, G. García Hernández, S. Gartner, Protocolo de diagnóstico y seguimiento de los pacientes con fibrosis quística, An. Españoles Pediatr. 50 (1999) 625–634. doi:10.1016/j.anpedi.2009.06.020.

[8] V.A. LeGrys, J.R. Yankaskas, L.M. Quittell, B.C. Marshall, P.J. Mogayzel, Diagnostic Sweat Testing: The Cystic Fibrosis Foundation Guidelines, J. Pediatr. 151 (2007) 85–89. doi:10.1016/j.jpeds.2007.03.002.

[9] M.D. Robert C. Stern, The diagnosis of cystic fibrosis, N. Engl. J. Med. 336 (1997) 487–491.

[10] B.J. Rosenstein, G.R. Cutting, The diagnosis of cystic fibrosis: A consensus statement, J. Pediatr. 132 (1998) 589–595. doi:10.1016/S0022-3476(98)70344-0.

[11] P.R. Sosnay, T.B. White, P.M. Farrell, C.L. Ren, N. Derichs, M.S. Howenstine, J.A. Nick, K. De Boeck, Diagnosis of Cystic Fibrosis in Nonscreened Populations, J. Pediatr. 181 (2017) S52–S57. doi:10.1016/j.jpeds.2016.09.068.

[12] W.A. Latzka, S.J. Montain, Water and electrolyte requirements for exercise. / Besoins en eau et electrolytes pour l'exercice., Clin. Sports Med. 18 (1999) 513–524. doi:10.1016/S0278-5919(05)70165-4.

[13] A.B. Stefaniak, C.J. Harvey, Dissolution of materials in artificial skin surface film liquids, Toxicol. Vitr. 20 (2006) 1265–1283. doi:10.1016/j.tiv.2006.05.011.

[14] G.T. Nagami, Hyperchloremia – Why and how, Nefrologia. 36 (2016) 347–353.

[15] G. Morrison, Serum Chloride., in: H.K. Walker, W.D. Hall, J.W. Hurst (Eds.), Clin. Methods Hist. Phys. Lab. Exam., 3rd ed., Boston: Butterworths, 1990: pp. 890–894.

[16] W.P. Mutter, C.A. Korzelius, Urine Chemistries, Hosp. Med. Clin. 1 (2012) e338–e352. doi:10.1016/j.ehmc.2012.04.007.

[17] R.W. Schrier, Diagnostic Value of Urinary Sodium, Chloride, Urea, and Flow, J. Am. Soc. Nephrol. 22 (2011) 1610–1613. doi:10.1681/ASN.2010121289.

[18] S. Watanabe, T. Kimura, K. Suenaga, S. Wada, K. Tsuda, S. Kasama, T. Takaoka, K. Kajiyama, M. Takeda, H. Yoshikawa, Decreased chloride levels of cerebrospinal fluid in patients with amyotrophic lateral sclerosis, J. Neurol. Sci. 285 (2009) 146–148. doi:10.1016/j.jns.2009.06.026.

[19] H.W. Doughty, Mohr's method for the determination of silver and halogens in other than neutral solutions, J. Am. Chem. Soc. 46 (1924) 2707–2709. doi:10.1021/ja01677a014.

[20] P. Díaz, Z. González, M. Granda, R. Menéndez, R. Santamaría, C. Blanco, Evaluating capacitive deionization for water desalination by direct determination of chloride ions, Desalination. 344 (2014) 396–401. doi:10.1016/j.desal.2014.04.013.

[21] R.G. Du, R.G. Hu, R.S. Huang, C.J. Lin, In situ measurement of Cl- concentrations and pH at the reinforcing steel/concrete interface by combination sensors, Anal. Chem. 78 (2006) 3179–3185. doi:10.1021/ac0517139.

[22] W.T. Grubb, Chloride - selective electrode, US3740326, 1973.

[23] A. Hulanicki, A. Michalska, All- solid- state chloride- selective electrode with poly(pyrrole) solid contact, Electroanalysis. 7 (1995) 692–693. doi:10.1002/elan.1140070718.

[24] J.S.F. Pereira, L.O. Diehl, F.A. Duarte, M.F.P. Santos, R.C.L. Guimarães, V.L. Dressler, É.M.M. Flores, Chloride determination by ion chromatography in petroleum coke after digestion by microwave-induced combustion, J. Chromatogr. A. 1213 (2008) 249–252. doi:10.1016/j.chroma.2008.10.079.

[25] A.M. Pimenta, A.N. Araújo, M.C.B.S.M. Montenegro, C. Pasquini, J.J.R. Rohwedder, I.M. Raimundo, Chloride-selective membrane electrodes and optodes based on an indium(III) porphyrin for the determination of chloride in a sequential injection analysis system, J. Pharm. Biomed. Anal. 36 (2004) 49–55. doi:10.1016/j.jpba.2004.04.011.

[26] H. Cao, D.H. Wu, Rapid and sensitive determination of trace chloride ion in drinks using resonance light scattering technique, J. Autom. Methods Manag. Chem. 2008 (2008) 0–5. doi:10.1155/2008/745636.

[27] R.B. Mesquita, S.M. Fernandes, A.O. Rangel, Turbidimetric determination of chloride in different types of water using a single sequential injection analysis system, J Env. Monit. 4 (2002) 458–461. doi:10.1039/b200456a.

[28] M.O. Gorbunova, A.V. Shevchenko, V.V. Apyari, A.A. Furletov, P.A. Volkov, A.V. Garshev, S.G. Dmitrienko, Selective determination of chloride ions using silver triangular nanoplates and dynamic gas extraction, Sensors Actuators, B Chem. 256 (2018) 699–705. doi:10.1016/j.snb.2017.09.212.

[29] A. Koh, D. Kang, Y. Xue, S. Lee, R.M. Pielak, J. Kim, T. Hwang, S. Min, A. Banks, M.C. Manco, L. Wang, K.R. Ammann, K. Jang, S. Han, R. Ghaffari, U. Paik, M.J. Slepian, Y. Huang, J.A. Rogers, A Soft, Wearable Microfluidic Device for the Capture, Storage, and Colorimetric Sensing of Sweat, Sci Transl Med. 8 (2017). doi:10.1126/scitranslmed.aaf2593.A.

[30] A. Martin, R. Narayanaswamy, Studies on quenching of fluorescence of reagents in aqueous solution leading to an optical chloride-ion sensor, Sensors Actuators B Chem. 39 (1997) 330–333. doi:10.1016/S0925-4005(97)80228-6.

[31] V.G. Bonifácio, L.C. Figueiredo-Filho, L.H. Marcolino, O. Fatibello-Filho, An improved flow system

for chloride determination in natural waters exploiting solid-phase reactor and long pathlength spectrophotometry, Talanta. 72 (2007) 663–667. doi:10.1016/j.talanta.2006.11.036.

[32] L.S. Laxmeshwar, M.S. Jadhav, J.F. Akki, P. Raikar, J. Kumar, O. prakash, R. Mahakud, U.S. Raikar, Quantification of chloride and iron in sugar factory effluent using long period fiber grating chemical sensor, Sensors Actuators B Chem. 258 (2018) 850–856. doi:10.1016/j.snb.2017.11.139.

[33] D.B. de Graaf, Y. Abbas, J.G. Bomer, W. Olthuis, A. van den Berg, Sensor-actuator system for dynamic chloride ion determination, Anal. Chim. Acta. 888 (2015) 44–51. doi:10.1016/j.aca.2015.06.047.

[34] D.H. Choi, Y. Li, G.R. Cutting, P.C. Searson, A wearable potentiometric sensor with integrated salt bridge for sweat chloride measurement, Sensors Actuators, B Chem. 250 (2017) 673–678. doi:10.1016/j.snb.2017.04.129.

[35] J. Bujes-Garrido, M.J. Arcos-Martínez, Development of a wearable electrochemical sensor for voltammetric determination of chloride ions, Sensors Actuators, B Chem. 240 (2017) 224–228. doi:10.1016/j.snb.2016.08.119.

[36] A. Cranny, N. Harris, N. White, Screen printed potentiometric chloride sensors, Procedia Eng. 87 (2014) 220–223. doi:10.1016/j.proeng.2014.11.626.

[37] V.A.T. Dam, M.A.G. Zevenbergen, R. van Schaijk, Toward wearable patch for sweat analysis, Sensors Actuators, B Chem. 236 (2016) 834–838. doi:10.1016/j.snb.2016.01.143.

[38] V.A.T. Dam, M.A.G. Zevenbergen, R. Van Schaijk, Flexible chloride sensor for sweat analysis, Procedia Eng. 120 (2015) 237–240. doi:10.1016/j.proeng.2015.08.588.

[39] V.A.T. Dam, M. Goedbloed, M.A.G. Zevenbergen, Solid-Contact Reference Electrode for Ion-Selective Sensors, Proceedings. 1 (2017) 464. doi:10.3390/proceedings1040464.

[40] I. Campos, R. Masot, M. Alcañiz, L. Gil, J. Soto, J.L. Vivancos, E. García-Breijo, R.H. Labrador, J.M. Barat, R. Martínez-Mañez., Accurate concentration determination of anions nitrate, nitrite and chloride in minced meat using a voltammetric electronic tongue, Sensors Actuators, B Chem. 149 (2010) 71–78. doi:10.1016/j.snb.2010.06.028.

[41] A.J. Bandodkar, J. Wang, Non-invasive wearable electrochemical sensors: A review, Trends Biotechnol. 32 (2014) 363–371. doi:10.1016/j.tibtech.2014.04.005.

[42] M. Bariya, H.Y.Y. Nyein, A. Javey, Wearable sweat sensors, Nat. Electron. 1 (2018) 160–171. doi:10.1038/s41928-018-0043-y.

[43] S. Emaminejad, W. Gao, E. Wu, Z.A. Davies, H. Yin Yin Nyein, S. Challa, S.P. Ryan, H.M. Fahad, K. Chen, Z. Shahpar, S. Talebi, C. Milla, A. Javey, R.W. Davis, Autonomous sweat extraction and analysis applied to cystic fibrosis and glucose monitoring using a fully integrated wearable platform, Proc. Natl. Acad. Sci. 114 (2017) 4625–4630. doi:10.1073/pnas.1701740114.

[44] W. Gao, S. Emaminejad, H.Y.Y. Nyein, S. Challa, K. Chen, A. Peck, H.M. Fahad, H. Ota, H. Shiraki, D. Kiriya, D.-H. Lien, G.A. Brooks, R.W. Davis, A. Javey, Fully integrated wearable sensor arrays for multiplexed in situ perspiration analysis, Nature. 529 (2016) 509–514. doi:10.1038/nature16521.

[45] G. Matzeu, L. Florea, D. Diamond, Advances in wearable chemical sensor design for monitoring biological fluids, Sensors Actuators, B Chem. 211 (2015) 403–418. doi:10.1016/j.snb.2015.01.077.

[46] J.R. Windmiller, J. Wang, Wearable Electrochemical Sensors and Biosensors: A Review, Electroanalysis. 25 (2013) 29–46. doi:10.1002/elan.201200349.

[47] M.H. Chiu, W.L. Cheng, G. Muthuraman, C.T. Hsu, H.H. Chung, J.M. Zen, A disposable screen-printed silver strip sensor for single drop analysis of halide in biological samples, Biosens. Bioelectron. 24 (2009) 3008–3013. doi:10.1016/j.bios.2009.03.004.

[48] J. Bujes-Garrido, M.J. Arcos-Martínez, Disposable sensor for electrochemical determination of chloride ions, Talanta. 155 (2016) 153–157. doi:10.1016/j.talanta.2016.04.038.

[49] O.D. Renedo, M.A. Alonso-Lomillo, M.J.A. Martínez, Recent developments in the field of screen-printed electrodes and their related applications, Talanta. 73 (2007) 202–219. doi:10.1016/j.talanta.2007.03.050.

[50] J. Bujes-Garrido, D. Izquierdo-Bote, A. Heras, A. Colina, M.J. Arcos-Martínez, Determination of halides using Ag nanoparticles-modified disposable electrodes. A first approach to a wearable sensor for quantification of chloride ions, Anal. Chim. Acta. 1012 (2018) 42–48. doi:10.1016/j.aca.2018.01.063.

[51] A.T. Kuhn, P.M. Wright, The behaviour of platinum, iridium and ruthenium electrodes in strong chloride solutions, J. Electroanal. Chem. 41 (1973) 329–349.

[52] S.B. Hall, E.A. Khudaish, A.L. Hart, Electrochemical oxidation of hydrogen peroxide at platinum

electrodes. Part V: inhibition by chloride, Electrochim. Acta. 45 (2000) 3573–3579.

[53] J. Gulens, Surface effects in relation to the response of solid-state ion-selective eletrodes, Ion-Selective Electrode Rev. 2 (1981) 117–157.

[54] J. Clavilier, The role of anion on the electrochemical behaviour of a {111} platinum surface; an unusual splitting of the voltammogram in the hydrogen region, J. Electroanal. Chem. 107 (1980) 211–216.

[55] J.A. Polta, D.C. Johnson, Pulsed Amperometric Detection of Electroinactive Adsorbates at Platinum Electrodes in a Flow Injection System, Anal. Chem. 57 (1985) 1373–1376.

[56] N. Priyantha, S. Malavipathirana, Effect of chloride irons on the electrochemical behaviour of platinum surfaces, J. Natl. Sci. Found. Sri Lanka. 24 (1996) 237–246. http://www.sljol.info/index.php/JNSFSL/article/view/5556.

[57] E.L. Littauer, L.L. Shreir, Anodic polarization of platinum in sodium chloride solutions, Electrochim. Acta. 11 (1966) 527–536.

[58] X.J. Huang, D.S. Silvester, I. Streeter, L. Aldous, C. Hardacre, R.G. Compton, Electroreduction of chlorine gas at platinum electrodes in several room temperature ionic liquids: Evidence of strong adsorption on the electrode surface revealed by unusual voltammetry in which currents decrease with increasing voltage scan rates, J. Phys. Chem. C. 112 (2008) 19477–19483. doi:10.1021/jp8082437.

[59] L. Sereno, V.A. Macagno, M.C. Giordano, Electrochemical Behaviour of the Chloride / Chlorine System At Platinum Electrodes in Acetonitrile Solutions, Electrochim. Acta. 17 (1972) 561–575.

[60] K. Murugappan, D.W.M. Arrigan, D.S. Silvester, Electrochemical Behavior of Chlorine on Platinum Microdisk and Screen-Printed Electrodes in a Room Temperature Ionic Liquid, J. Phys. Chem. C. 119 (2015) 23572–23579. doi:10.1021/acs.jpcc.5b07753.

[61] C.J. Harvey, R.F. LeBouf, A.B. Stefaniak, Formulation and stability of a novel artificial sebum under conditions of storage and use, Int. J. Cosmet. Sci. 32 (2010) 347–355. doi:10.1111/j.1468-2494.2010.00561.x.

[62] B. Molinero-Abad, D. Izquierdo, L. Pérez, I. Escudero, M.J. Arcos-Martínez, Comparison of backing materials of screen printed electrochemical sensors for direct determination of the sub-nanomolar concentration of lead in seawater, Talanta. 182 (2018) 549–557. doi:10.1016/j.talanta.2018.02.005.

[63] P. Daubinger, J. Kieninger, T. Unmüssig, G.A. Urban, Electrochemical characteristics of nanostructured platinum electrodes - a cyclic voltammetry study, Phys. Chem. Chem. Phys. 16 (2014) 8392–9. doi:10.1039/c4cp00342j.

[64] A.J. Bard, L.R. Faulkner, ELECTROCHEMICAL METHODS Fundamentals and Applications, 2nd Ed., John Wiley & Sons, Inc., 2001. doi:10.1016/B978-0-08-098353-0.00003-8.

[65] J. Mocak, a. M. Bond, S. Mitchell, G. Scollary, A statistical overview of standard (IUPAC and ACS) and new procedures for determining the limits of detection and quantification: Application to voltammetric and stripping techniques (Technical Report), Pure Appl. Chem. 69 (1997) 297–328. doi:10.1351/pac199769020297.

[66] E.R. Ziegel, Statistics and Chemometrics for Analytical Chemistry, 2004. doi:10.1198/tech.2004.s248.

[67] J.A. Polta, D.C. Johnson, The Direct Electrochemical Detection of Amino Acids at a Cu Electrode in an Acidic Chromatographic Effluent, J. Liq. Chromatogr. 6 (1983) 1727–1743.

Fig. 1. CV scans from -0.7 to 1.3 V recorded at SPPtE in a 200 µL drop of supporting electrolyte, containing 0, 1, 5, 10, 20, 30, 60, 80 and 100 mM of NaCl. Scan rate 0.1 V s^{-1}.

Fig. 2. SEM micrographs of the working SPPtE at three different magnifications.

Fig. 3. SPPtE sensor responses obtained in the optimal conditions. (a) CSV cathodic peaks recorded in a 200 µL drop of supporting electrolyte with chloride ranging from 0 to 150 mM; and (b) Average calibration curve and associated deviation, registered for seven distinct SPPtEs.

Fig. 4. Flexible Gore-Tex® SPPtEs-based sensors voltammetric peaks recorded in a 200 µL drop of synthetic sweat with chloride ranging from 0 to 150 mM, and respective average calibration curves for (◊) rigid polyester SPPtE and (□) Flexible Gore-Tex® SPPtEs (n=3).

Table 1. X-Ray elemental analysis of SPPtE surface at different steps of voltammetric analysis.

Step of analysis	*wt (%)*		
	Pt	O	Cl
SPPtE	89.26 ± 0.15	2.73 ± 0.10	0.00 ± 0.00
SPPtE/EP	85.94 ± 3.26	3.29 ± 0.25	0.00 ± 0.00
SPPtE/EP/E_{dep} 0 mM NaCl	88.33 ± 0.57	3.41 ± 0.55	0.00 ± 0.00
SPPtE/EP/E_{dep} 10 mM NaCl	88.46 ± 0.98	2.96 ± 0.50	0.50 ± 0.05
SPPtE/EP/E_{dep} 150 mM NaCl	87.67 ± 0.38	2.51 ± 0.15	0.80 ± 0.05
SPPtE/EP/E_{dep} 10 mM NaCl/CSV	90.64 ± 0.26	2.31 ± 0.20	0.00 ± 0.00
SPPtE/EP/E_{dep} 150 mM NaCl/CSV	88.98 ± 0.20	3.02 ± 0.26	0.00 ± 0.00

SPPtE - untreated electrode; SPPtE/EP – After electropolishing step (0.1 M of KNO_3); SPPtE/EP/E_{dep} – After the anodic deposition (1.5 V, 15 s) for 0, 10, and 150 mM of NaCl; SPPtE/EP/E_{dep}/CSV - After CSV (from 1.10 to 0.1 V at 0, 10 and 150 mM of NaCl).

Table 2. Chloride determination in different samples using potentiometric (Cl-ISE) and voltammetric (SPPtE) methods. Triplicates were performed for each sample analysis.

Samples	**Cl – ISE**	**SPPtE**
	[Cl^-] mM	[Cl^-] mM
Sea Water	613.15 ± 6.77	613.14 ± 9.66
Saline Solution	141.10 ± 3.10	141.35 ± 3.46
Wholemeal biscuits	44.29 ± 1.77	47.11 ± 2.76
Chicken Stock	134.00 ± 1.16	122.36 ± 10.10
Human Plasma	46.37 ± 1.41	47.13 ± 0.53
	126.98 ± 2.26	126.05 ± 4.10
Urine	63.67 ± 2.89	60.81 ± 4.88
Real Human Sweat	31.92 ± 2.93	30.76 ± 3.61

Highlights:

- SPPtE-based sensor takes advantage of Cl^- and Pt interactions.
- CSV at the SPPtE returns a well-defined voltammetric peaks for Cl^- monitoring.
- The sensor offers a simple Cl^- determination in different types of matrices.
- The device was transfer to flexible Gore-Tex® SPPtE sensor for sweat analysis.
- Flexible SPPtE is suitable for CF diagnosis and monitoring electrolyte loss.

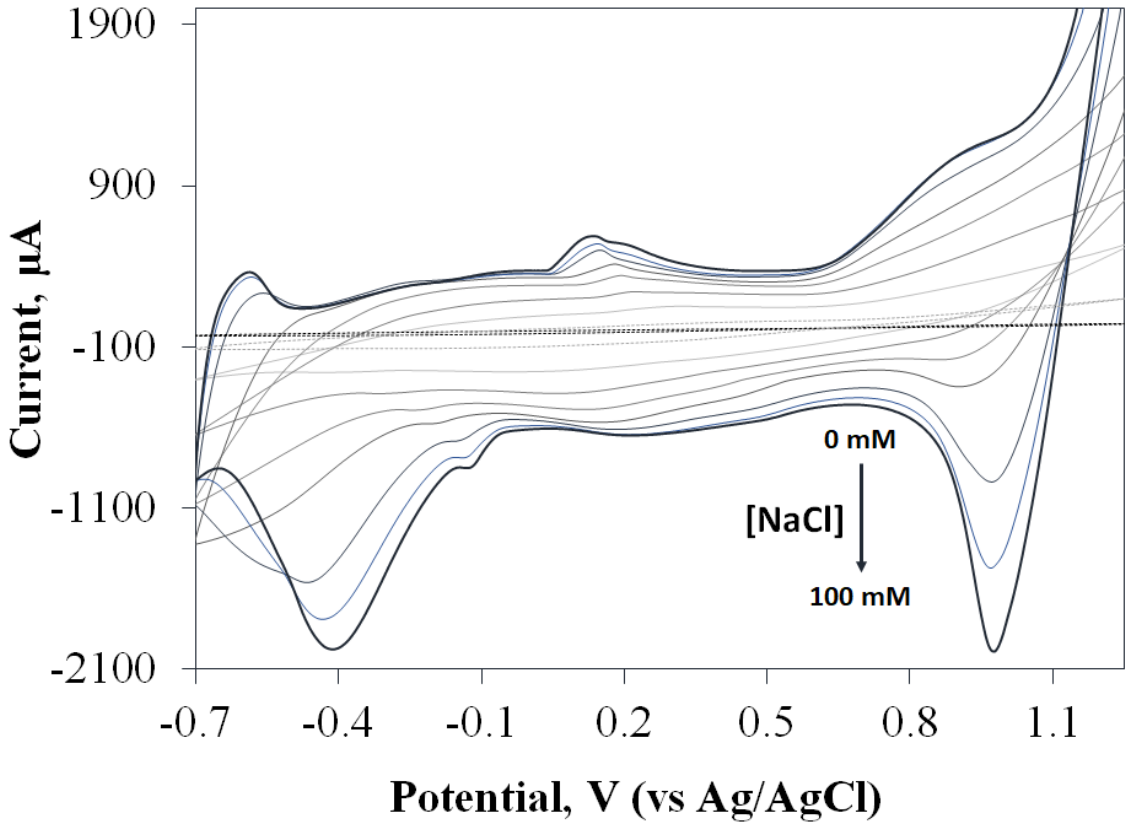

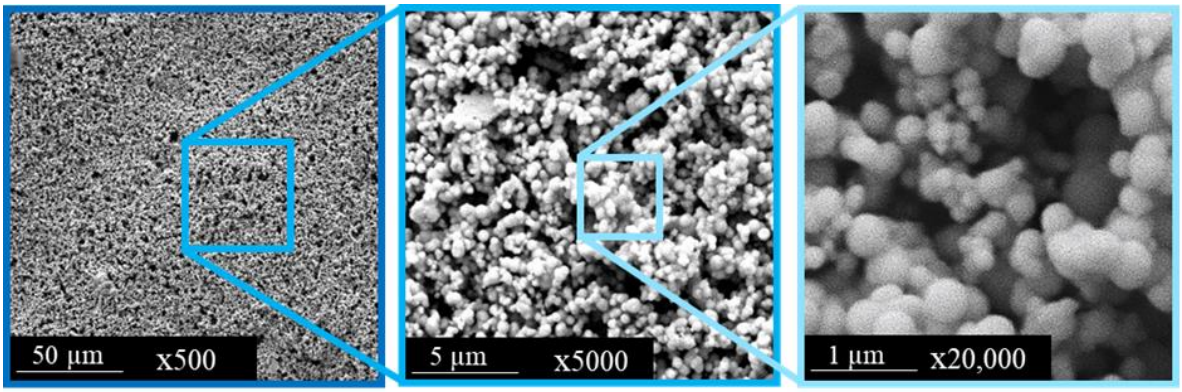
50 µm
x500
5 µm
x5000
1 µm
x20,000

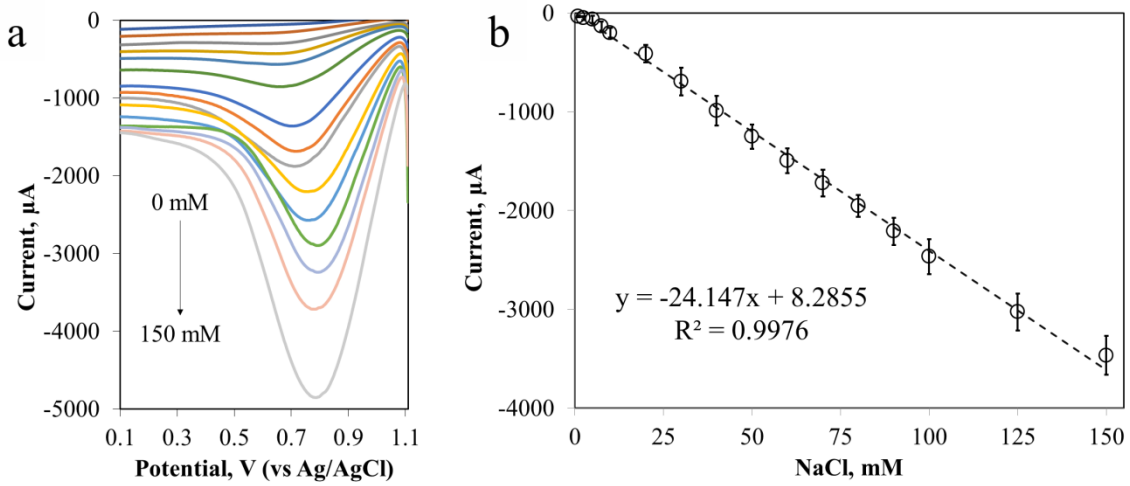
a
0
-1000
-2000
-3000
-4000
-5000
Current, µA
0 mM
150 mM
0.1
0.3
0.5
0.7
0.9
1.1
Potential, V (vs Ag/AgCl)
b
0
-1000
-2000
-3000
-4000
Current, µA
y = -24.147x + 8.2855
R² = 0.9976
0
25
50
75
100
125
150
NaCl, mM

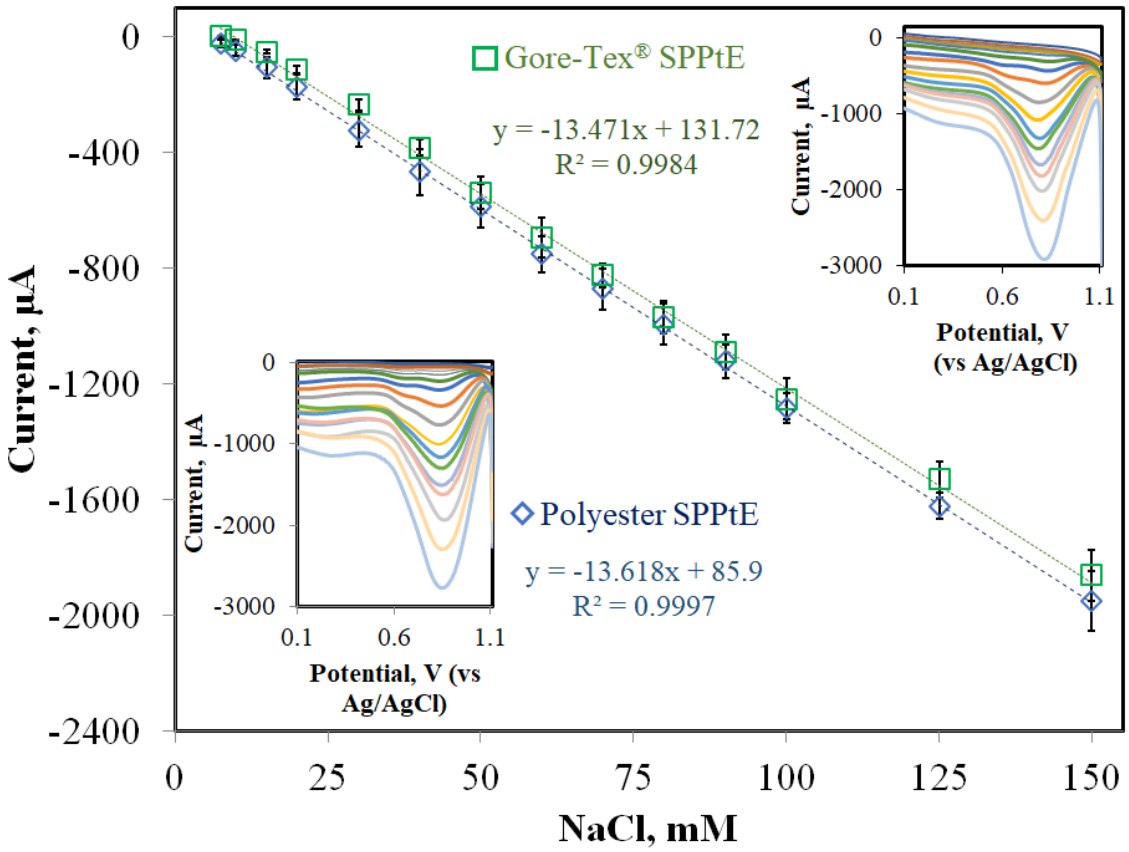
Gore-Tex® SPPtE
y = -13.471x + 131.72
R² = 0.9984
Polyester SPPtE
y = -13.618x + 85.9
R² = 0.9997
Current, µA
NaCl, mM
Potential, V (vs Ag/AgCl)
Potential, V (vs Ag/AgCl)
0
-400
-800
-1200
-1600
-2000
-2400
0
25
50
75
100
125
150
-1000
-2000
-3000
0.1
0.6
1.1